PROCEEDINGS OF SCIENCE

GAPS Detector Cooling System: Results from Antarctic Ground Tests

Kazutaka Aoyama[1,*] **on behalf of the GAPS collaboration**

[1]*Institute of Space and Astronautical Science, JAXA, Sagamihara, Japan*

E-mail: aoyama.kazutaka@jaxa.jp

The General Antiparticle Spectrometer (GAPS) experiment aims to elucidate the nature of dark matter by detecting low-energy antinuclei using a long-duration scientific balloon over Antarctica. The GAPS detector consists of a tracker made of lithium-drifted Silicon detectors, surrounded by two layers of Time-of-Flight (TOF) plastic scintillators. To achieve an energy resolution of 4 keV FWHM in the 20–100 keV range, the Silicon detectors are cooled to −40°C using Multi-loop Capillary Heat Pipes (MCHPs), specifically developed for GAPS. The MCHPs transport heat from the detectors to a radiator attached to the payload's sidewall. On the ground, the radiator is directly cooled by the Ground Cooling System (GCS) to enable detector testing. The GCS consists of a chiller, a cold plate, and insulating foam. GAPS has completed successful instrument commissioning during this past Antarctic launch season. During this period, we conducted cooling tests to investigate the detector performance using the GCS. Unfortunately, GAPS was not able to launch in the past season due to weather. GAPS remains assembled at the LDB site and stands ready for its first scientific ballon flight in the austral summer of 2025-2026. In this talk, we will present the results of the ground tests conducted during the 2024/25 season, with a particular focus on the performance of the cooling system.

39th International Cosmic Ray Conference (ICRC2025)
15–24 July 2025
Geneva, Switzerland

ICRC 2025
The Astroparticle Physics Conference
Geneva July 15-24, 2025

*Speaker

PoS(ICRC2025)466

1. Introduction

The General Antiparticle Spectrometer (GAPS) is a balloon-borne experiment designed to probe the nature of dark matter through the indirect detection of low-energy cosmic antinuclei, in particular antiprotons, antideuterons, and antihelium[1–3]. Among these, antideuterons serve as a particularly promising signal due to their extremely low expected astrophysical background at kinetic energies around 100 MeV/nucleon[4–6].

Unlike traditional cosmic-ray observation experiments that employ magnetic spectrometers to measure particle rigidity and charge, GAPS utilizes a unique detection approach based on exotic atom formation. When an antiparticle comes to rest in the detector material, it forms an exotic atom by replacing an electron. This atom de-excites by emitting a series of characteristic X-rays and then undergoes nuclear annihilation, producing a distinct set of secondary hadrons. This dual signature offers strong particle identification capability[7].

The GAPS detector consists of two main subsystems: a central tracker made of lithium-drifted silicon [Si(Li)] detectors and a surrounding Time-of-Flight (TOF) system composed of plastic scintillators[8–10]. The Si(Li) detectors act as both the stopping medium for antiparticles and as sensors for detecting X-rays and charged particles. To achieve the required energy resolution of 4 keV (FWHM) in the 20–100 keV range, Si(Li) detectors must be maintained at approximately −40°C. Accordingly, a dedicated thermal control system was developed to ensure stable operation in the stratosphere. The TOF system provides hit timing and position, as well as deposited energy. In addition, its signals are used for triggering. The entire payload is designed for launch aboard a NASA Long Duration Balloon (LDB) from Antarctica, where persistent circumpolar winds during the austral summer enable stratospheric flights of approximately 30 days under near-continuous solar illumination.

After completing comprehensive integration and validation campaigns in Japan and the United States, the Antarctic ground test served as the final full-system readiness check prior to launch. The first flight was scheduled for the 2024/2025 austral summer, but unfavorable winds and the early disappearance of the polar vortex prevented a launch attempt. This paper focuses on one of the key subsystems, thermal management of the Si(Li) detectors, and presents the results of ground testing conducted during the 2024/25 season.

2. Detector cooling system

2.1 Heat load to the Si(Li) detectors

During balloon flights, the Si(Li) detectors are subjected to two primary sources of heat: internal dissipation from the detectors and their associated electronics, and external environmental input. The internal heat primarily arises from the preamplifier circuit boards attached to each detector module, which contains four Si(Li) detectors wafers. The full tracker consists of a 6×6 array of modules, each stacked in 7 vertical layers and three layers of passive detectors providing target material. Although each board consumes only a small amount of power, the total internal heat load accumulates to approximately 90 W. In addition, the detectors are exposed to external thermal input from the surrounding environment. This contribution is highly variable, depending on atmospheric conditions, such as surface albedo. The external heat load is estimated to range from

80 to 180 W. As a result, the thermal control system must accommodate a total and dynamically varying heat load of 170–270 W to ensure stable operation of the detectors throughout the flight. In contrast, the heat load under ground-based conditions is expected to be higher than during balloon flight, due to differences in ambient temperature and atmospheric pressure.

2.2 Flight model design of cooling system

As with any balloon experiment, minimizing both power consumption and payload weight is mission critical. The cooling system must operate with minimal electrical power and be lightweight to meet flight constraints. To fulfill these requirements, the system employs multi-loop capillary heat pipes (MCHPs). This device passively transports heat without relying on consumable refrigerants such as liquid nitrogen, or on electrically powered cooling mechanisms, including mechanical pumps and cryocoolers. Instead, this approach relies on the principles of thermosiphons and oscillating heat pipes, offering an efficient and low-power thermal control.

The GAPS MCHP consists of 36 capillary loops connected in series, corresponding to the 36 module towers of the Si(Li) tracker. Each loop is embedded in an aluminum support structure that thermally interfaces with the Si(Li) detector modules. To enhance thermal coupling between the detector modules and the embedded heat pipes, thermal couplers are inserted between the Si(Li)-mounted aluminum plates and the heat pipe surface. The thermal conductance at this interface was empirically measured and incorporated into the thermal design. The working fluid used in the MCHP is R23, selected for its suitable thermophysical properties.

Figure 1 illustrates the thermal transport principle of the MCHP system and the overall heat flow path within the GAPS payload[11]. In the tracker region (heating section), heat is absorbed by the two-phase working fluid contained with the MCHP. This fluid transports heat via both latent and sensible heat. The vaporized fluid flows through the upper adiabatic section toward the radiator, where it condenses and releases heat to the environment (cooling section). The condensed liquid returns through the lower adiabatic section to the tracker region of the next loop, thereby completing the passive heat transfer cycle. To ensure stable and reliable operation, the MCHP system includes a dedicated fluid reservoir. The reservoir temperature is controlled by a feedback-regulated heater, which determines the saturation pressure of the working fluid and stabilizes the operating point, as illustrated in Fig. 1(b). The reservoir also acts as a buffer, automatically adjusting the fluid volume within the main loop in response to changes in heat load.

To monitor the thermal behavior of the cooling system in real time, Resistance Temperature Detectors (RTDs) are mounted along the surface of the MCHPs[12]. These sensors provide continuous measurements of the temperature distribution along the thermal path from the Si(Li) detector modules to the radiator. Figure 2 presents representative temperature profiles recorded by the RTDs before and after the cooling of the Si(Li) detectors during ground-based testing. This real-time monitoring is essential for verifying uniform heat transport performance and identifying any localized thermal anomalies during both ground-based testing and flight operations.

3. Ground cooling system

A comprehensive functional check of the entire GAPS payload is essential before flight. This includes verifying that the detectors can reach and maintain their target operating temperature and

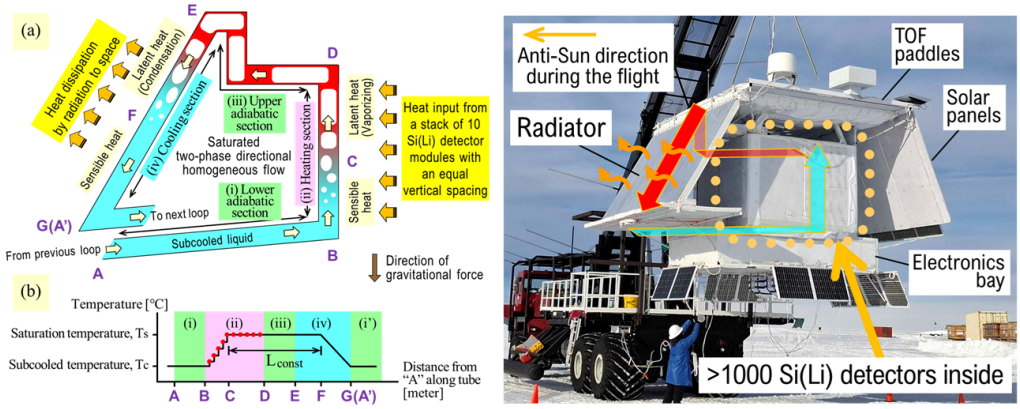

Figure 1: Left: Schematic diagram of the MCHP operating principle in the GAPS system. Under two-phase conditions, the working fluid maintains a constant temperature, which is equal to the reservoir temperature. This diagram is obtained from Ref.[12] Right: Photograph of the GAPS payload overlaid with the routing of the heat pipe loops from the Si(Li) tracker to the radiator, which measures 4 m in width and 2.3 m in height.

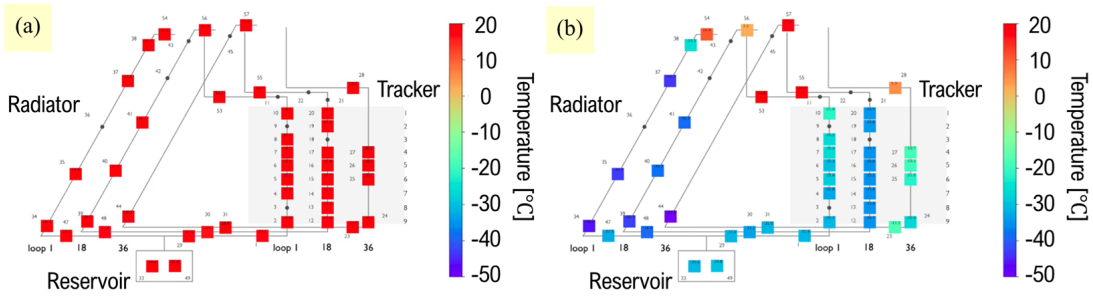

Figure 2: Representative temperature distributions measured by onboard RTDs along three MCHP loops: (a) before and (b) after the Si(Li) detector cooling. Data were obtained during thermal validation tests on the ground at Nevis Laboratories, Columbia University.

that the thermal system can effectively transport heat from the detectors to the radiator. Unlike at high altitudes, radiative cooling is ineffective on the ground due to the higher density of atmosphere and the limited view factor to cold space, making it difficult to sufficiently cool the radiator through radiation alone. Furthermore, performing such tests on the ground presents practical limitations. Large vacuum thermal chambers are not available in Antarctica, and modifying the gondola configuration for test purposes is undesirable.

To overcome these constraints, a dedicated Ground Cooling System (GCS) was developed[13]. The GCS consists of three main components, as shown in Fig.3: a commercial chiller, a cold plate, and thermal insulation. The chiller circulates a coolant fluid through the cold plate, which is attached and thermally coupled to the external surface of the radiator. The cold plate maintains the radiator at a target temperature well below the ambient temperature. This setup simulates the thermal boundary conditions that would otherwise be provided by radiative cooling in the stratosphere. To minimize heat load, the radiator and surrounding structures are enclosed in Styrofoam.

Figure 3: Photograph of the Ground Cooling System (GCS) setup. The system includes a commercial chiller, a cold plate attached to the radiator surface, and Styrofoam insulation to reduce environmental heat load.

4. Ground test in Antarctica

During the Antarctic summer season of 2024/25, the GAPS team conducted full-scale integration and test operations on the ground at the Long Duration Balloon (LDB) site near McMurdo Station. The entire thermal system was continuously operated for nine days to confirm readiness for flight.

Figure 4 presents the temperature history of the heat pipe loop that is expected to have the largest heat load. Figure 4(a) shows the temperatures recorded at four vertical positions along the tracker: 0 cm (purple), 50 cm (blue), 70 cm (green), and 90 cm (red) height from the bottom of tracker region. Figure 4(b) displays the temperatures at the top (magenta) and bottom (cyan) of the radiator. The reservoir temperature (black line) and the ambient air temperature (gray line) are also plotted in both panels. While the temperatures of the radiator vary depending on external thermal conditions, the tracker region maintains a nearly constant temperature, demonstrating effective thermal isolation and control. As expected, the temperature in the tracker region was higher (around -30°C) than the target operational value (near -40°C), due to enhanced convective heat transfer and a relatively high radiator temperature (approximately -50°C) during the ground operation. We expect that the radiator temperature can reach below -65°C during the flight, allowing the tracker region to approach the target temperature of -40°C. Notably, we achieved approximately -40°C in the tracker during the integration test at Nevis Laboratories, Columbia University, when the radiator temperature was lower.

Figure 5 shows the temperature distribution along the heat pipe. The horizontal axis represents the RTD index from the radiator outlet toward the tracker. The red line corresponds to a "hot case," characterized by higher ambient temperatures and environmental heat load. The blue line represents a "cold case", under lower ambient temperatures and heat load. Figure 5(a) corresponds to the loop expected to receive the highest heat load, whereas Figure 5(b) shows the one expected to receive the lowest. Figure 5(a) and Figure 4 show data from the same loop. Although temperature gradients appear near the radiator, the tracker region maintains a nearly uniform and stable temperature in

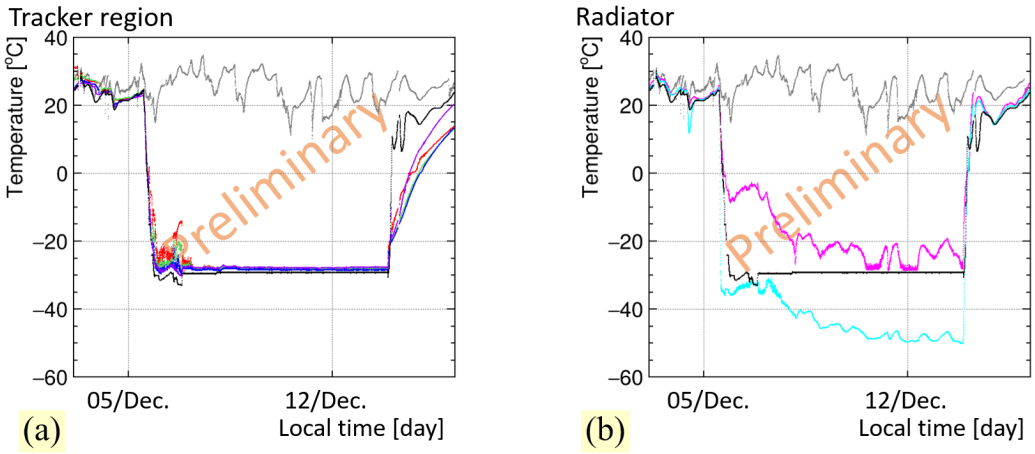

Figure 4: Time history of temperatures during the nine-day operation test. (a) Temperatures measured at four vertical locations along the tracker structure, 0 cm (purple), 50 cm (blue), 70 cm (green), and 90 cm (red) from the bottom. (b) Temperatures measured at the top (magenta) and bottom (cyan) of the radiator. Black and gray lines indicate the reservoir and ambient air temperatures, respectively. As expected, tracker temperatures remained around −30°C, above the target of −40°C, due to limited radiator cooling (−50°C) during the ground operation. In ground tests at Nevis Lab, −40°C was achieved with lower radiator temperature. Radiator temperatures below −65°C are expected during the flight to enable the tracker region to reach its target temperature.

both cases. Both the stability and uniformity of the temperature are essential for reliable Si(Li) detector operation.

5. Conclusion

The GAPS experiment employs a novel thermal management system using multi-loop capillary heat pipes (MCHPs) to passively cool the array of Si(Li) detectors in the stratospheric environment. This system is designed to maintain detector temperatures near −40°C with minimal power consumption and structural mass, which are critical constraints for long-duration balloon missions.

To perform the final readiness check, a 2024/25 ground testing campaign was conducted at the Antarctic LDB site during the 2024/25 austral summer. The dedicated GCS was developed to perform the cooling test without modifying the gondola configuration or relying on large-scale vacuum facilities.

Throughout the nine-day test, the MCHP system demonstrated robust thermal control. As expected, the tracker temperature was above the target temperature during the ground operation, due to limited radiator cooling and enhanced convective heat transfer under test conditions. At high altitude, where the radiator is expected to reach below −65°C and convective heat transfer is significantly reduced, the tracker region is expected to reach its operational target temperature. In addition, real-time RTD monitoring confirmed uniform heat transport and effective thermal regulation along the entire heat path from the detector modules to the radiator.

Prior to deployment to Antarctica, all integration, and subsystem-level validation were completed in the United States and Japan. The Antarctic ground operation served as the final end-to-end

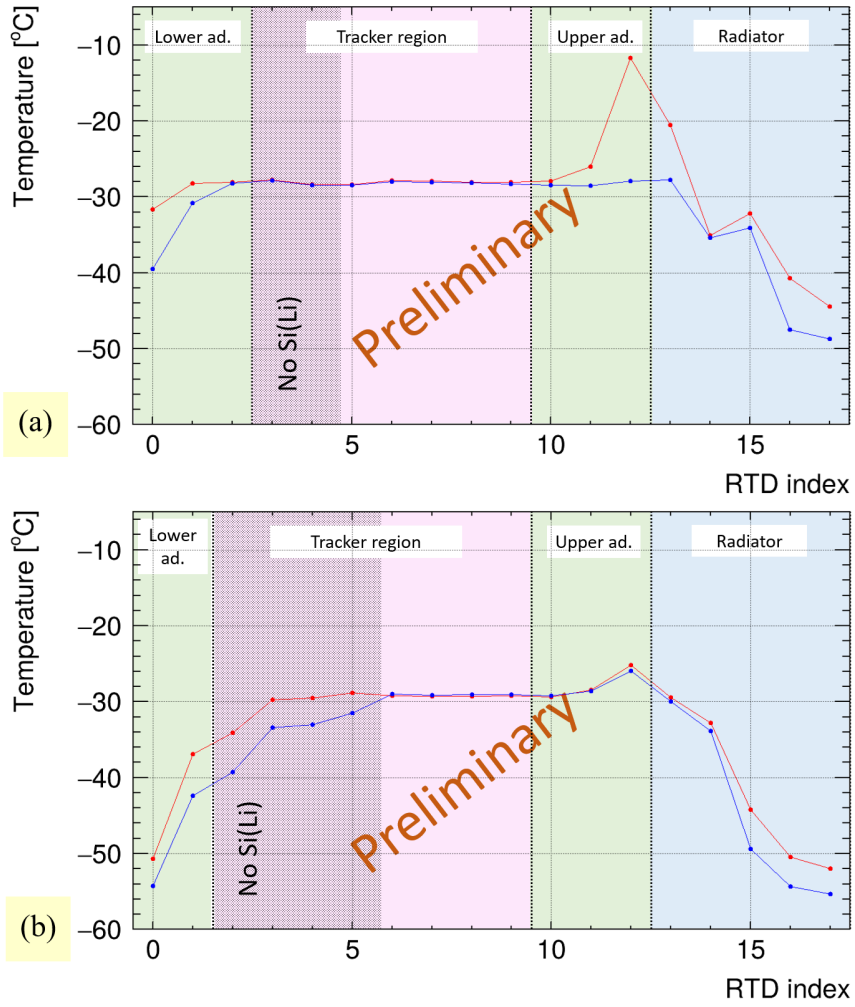

Figure 5: Temperature distribution along the heat pipe loop measured by RTDs. (a) The loop expected to have the highest heat input. (b) The loop expected to have the lowest heat input. Red lines correspond to a "hot case" with relatively high ambient temperature and large environmental heat input; blue lines represent a "cold case" under lower ambient temperature conditions. While temperature differences are observed near the radiator, the tracker region maintains nearly constant temperature in both cases, demonstrating stable and uniform thermal control.

operational test to confirm flight readiness before flight. The successful operation of the GCS and the thermal subsystem on the Antarctic ground confirmed readiness for flight. Unfortunately, GAPS was not able to launch in the past season due to weather. GAPS remains assembled at the LDB site and stands ready for its first scientific ballon flight in the austral summer of 2025-2026.

Acknowledgments

This work is supported in the U.S. by NASA Astrophysics Research and Analysis GAPS grants(NNX17AB44G, NNX17AB46G, NNX17AB47G, 80NSSC21K1877) PI, C. Hailey, in Japan by JAXA/ISAS Small Science Program FY2017, and in Italy by Istituto Nazionale di Fisica Nucleare (INFN) and by the Italian Space Agency through the ASI INFN agreement n. 2018-28-HH.0:

"Partecipazione italiana al GAPS - General AntiParticle Spectrometer". H. Fuke is supported by JSPS KAKENHI grants (JP17H01136, JP19H05198, JP22KK0042, and JP22H00147). K. Perez, G. Bridges, K. Pappas, and S. Vickers are also supported by Heising-Simons Foundation awards 2023-4617 and 2025-6055. R. A. Ong receives support from the UCLA Division of Physical Sciences. This work is partially supported by the U.S. Department of Energy, Office of Science under contract number DE-AC05-00OR22725. Sydney Feldman was supported through the National Science Foundation Graduate Research Fellowship under grant 2034835. The contributions of C. Gerrity were supported by NASA under award No. 80NSSC19K1425 of the Future Investigators in NASA Earth and Space Science and Technology (FINESST) program. K. Yee is supported through the National Science Foundation Graduate Research Fellowship under grant 2141064. K. Aoyama receives support from JSPS KAKENHI grant JP24K22891. K. Mizukoshi receives support from JSPS KAKENHI grants (JP22K20375 and JP24K17079). S. Okazaki receives support from JSPS KAKENHI grants (JP18K13928 and JP22KK0042). Y. Shimizu receives support from JSPS KAKENHI grants (JP20K04002, JP22KK0042, JP23K03436). M. Xiao, Z. Wu and J. Yang receive support from Yangyang Development Fund. The technical support and advanced computing resources from University of Hawaii Information Technology Services – Research Cyberinfrastructure, funded in part by the National Science Foundation CC* awards # 2201428 and # 2232862 are gratefully acknowledged. This research was done using services provided by the OSG Consortium [14–17], which is supported by the National Science Foundation awards #2030508 and #2323298. We express our sincere thanks to the NASA Columbia Scientific Balloon Facility and the National Science Foundation United States Antarctic Program for their professional support throughout the balloon flight preparation.

References

[1] F. Rogers et al., Astropart. Phys. **145** (2023), 102791.
[2] T. Aramaki et al., Astropart. Phys. **74** (2016) p 6-13.
[3] N. Saffold et al., Astropart. Phys. **130** (2021), 102580.
[4] P. von Doetinchem et al., J. Cosmol. Astropart. Phys. **08** (2020) 035.
[5] F. Donato, N. Fornengo, and P. Salati, Phys. Rev. D **62** (2000) 043003.
[6] M. Korsmeier, F. Donato, N. Fornengo, Phys. Rev. D **97** (2018) 103011.
[7] C.J. Hailey, New Journal of Physics **11** (2009) 105022.
[8] M. Kozai et al., Nucl. Instrum. Methods Phys. Res. A **947** (2019) 1662695.
[9] M. Xiao et al., IEEE Transactions on Nuclear Science **8** (2023) 2125.
[10] S.N. Feldman et al., Proceedings of Science Volume 444 - ICRC2023.
[11] H. Fuke et al., Nucl. Instrum. Methods Phys. Res. **1049** (2023) 168102.
[12] M. Kozai et al., 44th COSPAR Scientific Assembly, Athens (2022) TF-278.
[13] H. Fuke et al., Journal of Evolving Space Activities **1** (2023) 2.
[14] R. Pordes et al., *J. Phys. Conf. Ser.* **78** (2007) 012057.
[15] I. Sfiligoi et al., *2009 WRI World Congress on Computer Science and Information Engineering* **2** (2009) 428–432.
[16] OSG, *OSPool* (2006)
[17] OSG, *Open Science Data Federation* (2015)

Full Authors List: GAPS Collaboration

K. Aoyama[1], T. Aramaki[2], P. Beggs[3], M. Boezio[4,5], S. E. Boggs[6], G. Bridges[7], V. Bonvicini[4], D. Campana[8], E. Everson[3], L. Fabris[9], S. Feldman[3], H. Fuke[1], F. Gahbauer[7], C. Gerrity[10], L. Ghislotti[11,12], C. J. Hailey[7], T. Hayashi[3], A. Kawachi[13], K. Konoma[13], M. Kozai[25], P. Lazzaroni[11], A. Lowell[14], M. Manghisoni[11,12], M. Martucci[15], K. Mizukoshi[17], E. Mocchiutti[4], B. Mochizuki[14], K. Munakata[18], R. Munini[4,5], S. Okazaki[26], R. A. Ong[3], G. Osteria[8], F. Palma[15], K. Pappas[7], K. Perez[7], F. Perfetto[8,19], L. Ratti[11,12], V. Re[11,12], E. Riceputi[11,12], F. Rogers[14], S. Sakamoto[20], P. Sawant[15,16] V. Scotti[8,19], Y. Shimizu[20], R. Sparvoli[15,16], A. Stoessl[10], A. Suraj[2], A. Tiberio[21,22], G. Tytus[10], E. Vannuccini[21], S. Vickers[7], P. von Doetinchem[10], L. Volpicelli[15,16], Z. Wu[23], M. Xiao[23], J. Yang[23], K. Yee[7,24], T. Yoshida[1], G. Zampa[4], J. Zeng[2], and J. Zweerink[3]

[1]Institute of Space and Astronautical Science, Japan Aerospace Exploration Agency (ISAS/JAXA), Sagamihara, Kanagawa 252-5210, Japan. [2]Northeastern University, 360 Huntington Avenue, Boston, MA 02115, USA. [3]University of California, Los Angeles, Los Angeles, CA 90095, USA. [4]INFN, Sezione di Trieste, I-34149 Trieste, Italy. [5]IFPU, I-34014 Trieste, Italy. [6]University of California, San Diego, La Jolla, CA 90037, USA. [7]Columbia University, New York, NY 10027, USA. [8]INFN, Sezione di Napoli, I-80126 Naples, Italy. [9]Oak Ridge National Laboratory, Oak Ridge, TN 37831, USA. [10]University of Hawaii at Manoa, Honolulu, HI 96822 USA. [11]INFN, Sezione di Pavia, I-27100 Pavia, Italy. [12]Universitá di Bergamo, I-24044 Dalmine (BG), Italy. [13]Tokai University, Hiratsuka, Kanagawa 259-1292, Japan. [14]Space Sciences Laboratory, University of California, Berkeley, 7 Gauss Way, Berkeley, CA 94720, USA. [15]INFN, Sezione di Rome "Tor Vergata", I-00133 Rome, Italy. [16]Universitá di Roma "Tor Vergata", I-00133 Rome, Italy. [17]Tohoku University, Aoba-6-3 Aramaki, Aoba Ward, Sendai, Miyagi 980-8578, Japan. [18]Shinshu University, Matsumoto, Nagano 390-8621, Japan. [19]Universitá di Napoli "Federico II", I-80138 Naples, Italy. [20]Kanagawa University, Yokohama, Kanagawa 221-8686, Japan. [21]INFN, Sezione di Firenze, I-50019 Sesto Fiorentino, Florence, Italy. [22] Universita' degli Studi Firenze, 50121 Firenze FI, Italy [23] School of Physics and Astronomy, Shanghai Jiao Tong University, Key Laboratory for Particle Astrophysics and Cosmology (MoE), Shanghai Key Laboratory for Particle Physics and Cosmology, 800 Dongchuan RD. Minhang District, Shanghai 200240, China [24]Massachusetts Institute of Technology, Cambridge, MA 02139, USA. [25]Research Organization of Information and Systems, 4 Chome-3-13 Toranomon, Minato City, Tokyo 105-0001, Japan. [26]Research and Development Directorate, Japan Aerospace Exploration Agency, Tsukuba, Ibaraki 305-8505, Japan.

PoS(ICRC2025)466